Heliyon 10 (2024) e27828

Contents lists available at ScienceDirect

Heliyon

journal homepage: www.cell.com/heliyon

Research article

Antithrombotic pharmacodynamics and metabolomics study in raw and processed products of *Whitmania pigra* Whitman

Hongqian Kui [a], Yan Lei [a], Chunxue Jia [a], Quancheng Xin [a], Rustam Tursun [a], Miao Zhong [a], Chuanxin Liu [a,b,**], Ruijuan Yuan [a,*]

[a] *School of Chinese Materia Medica, Beijing University of Chinese Medicine, China*
[b] *Department of Metabolism and Endocrinology, Endocrine, and Metabolic Disease Center, The First Affiliated Hospital, and College of Clinical Medicine of Henan, University of Science and Technology, Medical Key Laboratory of Hereditary Rare Diseases of Henan, Luoyang Sub-center of National Clinical Research Center for Metabolic Diseases, Luoyang, China*

ARTICLE INFO

Keywords:
Whitmania pigra Whitman
Leech
Antithrombotic
Processed traditional Chinese medicine
Metabolomics

ABSTRACT

Objective: As a traditional Chinese medicine, leech has obvious pharmacological activities in anticoagulantion and antithrombosis. *Whitmania pigra* Whitman (WP) is the most commonly used leech in the Chinese market. It is often used in clinical applications after high-temperature processing by talcum powder to remove the fishy taste and facilitate crushing. The anticoagulant and thrombolytic active ingredients are protein and polypeptide, which may denaturate and lose activity after high-temperature processing. The rationality of its processing has been questioned in recent years. This study aims to investigate the effect of talcum powder scalding on the antithrombotic activity of WP *in vivo* and to discuss its pharmacodynamic mechanism *in vivo*.
Methods: Raw and talcum-powdered processed WP were administered intragastrically for 14 days, and carrageenan was injected intraperitoneally to prepare a mouse model of tail vein thrombosis. The incidence rate of tail vein thrombosis and the thrombus area under pathological tissue sections were calculated to evaluate the antithrombotic effect between raw and processed WP. Non-targeted metabolomics was conducted using UPLC-Q-TOF/MS technology to analyze the changes of small molecule metabolites in the body after administration of WP.
Results: After intragastric administration, both the raw product and the processed product of WP could inhibit the thrombosis induced by carrageenan, and the processed product had a more apparent antithrombotic effect than the raw product. The administration of WP could regulate the changes of some small molecular metabolites, such as amino acids, lipids, and steroids, in Sphingolipid metabolism and Glycerophospholipid metabolism.
Conclusions: Based on the results of pharmacodynamics and metabolomics, processed WP will not reduce the antithrombotic activity of WP. This study provided a scientific basis for the rational use of leeches.

Abbreviations: WP, *Whitmania pigra* Whitman; EDTA, Ethylene Diamine Tetraacetic Acid; QC, Quality Control; RSD, Relative Standard Deviation; BPC, Base Peak Chromatogram; PCA, Principal Component Analysis; OPLS-DA, Orthogonal Partial Least Squares-Discriminant Analysis; VIP, Variable Importance in Protection.

* Corresponding author. School of Chinese Materia Medica, Beijing University of Chinese Medicine, Northeast Corner of the Intersection of Yangguang South Street and Baiyang East Road, Fangshan District, Beijing, 102488, China.
** Corresponding author. The First Affiliated Hospital of Henan University of Science and Technology, 24th, Jinghua Road, Jianxi District, Luoyang, 471003, China.
E-mail addresses: 15222003775@163.com (C. Liu), rjyuance@126.com (R. Yuan).

https://doi.org/10.1016/j.heliyon.2024.e27828
Received 4 August 2023; Received in revised form 6 March 2024; Accepted 7 March 2024
Available online 19 March 2024

1. Introduction

Leech is a traditional Chinese medicine for promoting blood circulation and removing blood stasis. It was first recorded in "Shen Nong's Herbal Classic" (about 100 B. C.) and has been used for thousands of years. According to Chinese Pharmacopeia, leeches have the effects of dredging blood vessels and dissipating congestion [1]. Modern pharmacological results have shown that leeches have effects such as anticoagulation [2], antithrombosis [3], antiplatelet aggregation [4], regulating blood lipids, and improving abnormal blood rheology [5], etc. They are widely used in the treatment of diseases such as hypertension and hyperlipidemia. Three leech species, including *Whitmania pigra* Whitman (WP), *Hirudo nipponia* Whitman, and *Whitmania acranulata* Whitman, were recorded in the 2020 edition of "Chinese Pharmacopeia." According to their feeding habits, they can be divided into blood-sucking leeches and non-blood-sucking leeches. The former suck the blood of humans and animals, and the common specie is *Hirudo nipponia* Whitman. The latter feeds on molluscs such as snails and river mussels, and the common species is WP.

The active anticoagulant ingredients in leeches can be divided into two categories; one is protease inhibitors, the other is ingredients that directly act on thrombin, such as hirudin. Hirudin is secreted in the saliva of leeches during sucking blood to prevent blood coagulation, which is the strongest thrombin inhibitor found so far [6–8]. Therefore, blood-sucking leeches were significantly more active than non-blood-sucking leeches. As a non-blood-sucking leech, WP has not been reported to contain hirudin analogues. Despite this, WP is currently used as the mainstream species in the Chinese market due to its bigger body weight and higher yield than blood-sucking leeches.

Leeches have a terrible fishy smell that is difficult to take orally, and they are flexible in texture that is difficult to crush into powder. In order to remove the fishy taste and facilitate crushing, they were usually used after processing since the Han Dynasty. High-temperature scalding with talcum powder has been the mainstream processing method from ancient times to the present. In recent years, the rationality of leech processing has been questioned. Many scholars believe that processing under high temperatures would lead to the inactivation of active proteins. At the same time, high-temperature processing could cause protein denaturation, leading to a decrease in protein solubility. So, they advocated that leeches should be used raw [9]. However, the rationality of leech processing should be deeply studied due to their different active ingredients between different leeches. For blood-sucking leeches, their main active ingredient, hirudins, is easily destroyed at high temperatures, so it is suitable for using raw materials [10]. However, the WP's active ingredient is not the hirudin secreted in the saliva but the proteins or peptides in the leech body [11]. WP is usually orally administered after decoction. The peptides degraded by various digestive enzymes in the digestive tract after oral administration may be the active ingredients that really exert anticoagulant effects. After high-temperature processing, the active peptides may more easily released from the denatured proteins [12,13]. So, the rationality of high-temperature processing for WP may be different with blood-sucking leeches. Still, its pharmacodynamics and mechanism *in vivo* need to be further studied.

In order to explore the effect of talcum powder scalding on the antithrombotic activity of leeches *in vivo*. In this study, WP, the most commonly used leech in the Chinese market, was taken as the research object. Raw and processed WP was orally administered, and carrageenan was injected intraperitoneally to prepare a mouse model of tail vein thrombosis. The pharmacodynamics was evaluated based on the incidence rate of tail vein thrombosis and thrombus area. And non targeted metabolomics was studied using UPLC-Q-TOF/MS technology to explore the antithrombotic mechanism of raw and processed WP. This study provided a theoretical basis for the rational use of leeches.

2. Materials and methods

2.1. Instruments

ACQUITY Ultra-High Performance Liquid Chromatography (Waters, USA), SYNAPT G2-Si Q-TOF/MS Quadrupole Time-of-flight Mass Spectrometer (Waters, USA), Ultra-High-Speed Low-Temperature refrigerated centrifuge (Shanghai Anting Scientific Instrument Factory), ME155DU electronic balance (Shanghai Mettler-Toledo Instrument Co., Ltd.), KQ-300DB CNC ultrasonic cleaner (Kunshan Ultrasonic Instrument Co., Ltd.).

2.2. Herbs and reagents

Raw *Whitmania pigra* Whitma (dry product, Beijing Tongrentang Co., Ltd, B/N: 170319) from the market was identified by Associate Professor Zhenfang Bai of the College of Chinese Materia Medica, Beijing University of Chinese Medicine; Talcum powder (Beijing Shuangqiao Yanjing Chinese Herbal Pieces Factory, China, B/N: 1608009); Carrageenan (Shanghai Yuanye Biotechnology

Table 1
Administration dose and regimen.

Group	Number	Drug	Dose	Administration	Duration
Control	12	0.9% NaCl	0.2 mL/d	i.g.	16 d
Model	12	0.9% NaCl	0.2 mL/d	i.g.	16 d
Positive Drug	12	Aspirin	200 mg/kg/d	i.g.	16 d
Raw WP products	12	*Whitmania pigra* Whitman water-hanging dry product coarse powder	200 mg/kg/d	i.g.	16 d
Processed WP products	12	*Whitmania pigra* Whitman talcum powder scalding product coarse powder	200 mg/kg/d	i.g.	16 d

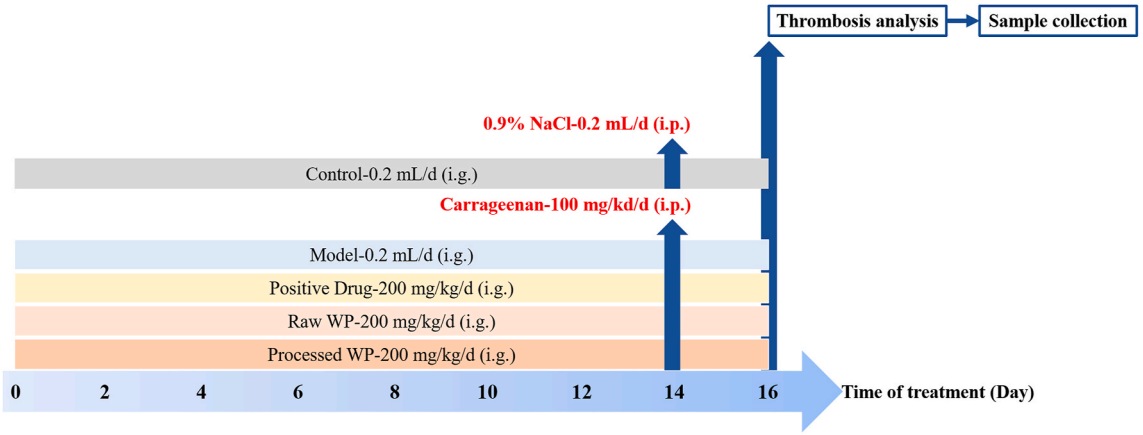

Fig. 1. Experimental design.

Co., Ltd., China, B/N: 181109); Aspirin (Sigma-Aldrich, St. Louis, MO, USA, B/N: S17061); Mass spectrometry grade methanol, acetonitrile and formic acid (Thermo Fisher Scientific (China) Co., Ltd., China); ultrapure water (Guangzhou Watsons Food and Beverage Co., Ltd., China).

2.3. Animals

ICR mice (male, SPF grade, 25–30 g) were purchased from Sibeifu (Beijing) Biotechnology Co., Ltd. and raised in the Animal Laboratory of Liangxiang Campus, Beijing University of Chinese Medicine. The feeding room alternates day and night with a 12-h cycle; the ambient temperature is 23 ± 2 °C, and the humidity is 35 ± 5%. Food and water are freely available during the feeding period. All animal care and experimental procedures followed the Regulations of the People's Republic of China on the Administration of Experimental Animals, and all animal experiments were approved by the Animal Ethics Committee of Beijing University of Chinese Medicine (No. BUCM-4-2022010102-1109, No. BUCM-4-2022010103-1110). After the experiment, all animals were anesthetized with 2% isoflurane inhalation, and the animals were sacrificed by cervical dislocation for euthanasia. In order to protect animals used for scientific purposes, all animal experimentation procedures comply with the guidelines of EU Directive 2010/63/EU on animal experimentation.

2.4. Pretreatment of WP samples

2.4.1. Preparation of raw WP powder

Take an appropriate amount of raw WP, crush it into powder, and pass it through a No. 4 medicine sieve to obtain a coarse raw WP powder. Store it in a sealed container at - 20 °C.

2.4.2. Preparation of processed WP powder

Put an appropriate amount of talcum powder in the pot, fry it with strong fire until it is in a flexible state, pour a few raw WP into talcum powder, and fry them until they bulge slightly. Take out the WP, brush off the talcum powder, crush it into powder, pass it through a No. 4 medicine sieve to obtain the coarse powder of processed WP, and store it in a sealed container at −20 °C.

2.5. Solution preparation

2.5.1. Preparation of WP sample solution

Respectively weigh an appropriate amount of raw WP and processed WP coarse powder, add normal saline, and stir evenly. It can be prepared into a drug solution suspension of WP with 0.1 g/mL concentration.

2.5.2. Preparation of carrageenan solution

Weigh an appropriate amount of carrageenan and add normal saline to prepare a solution with a mass fraction of 0.5%. This solution is prepared to use immediately.

2.5.3. Preparation of aspirin solution

Immediately before use, an appropriate amount of aspirin was weighed and added to 0.5% CMC-Na solution to prepare an aspirin drug solution suspension with 0.01 g/mL concentration.

2.6. Antithrombotic pharmacodynamics study in raw and processed WP

2.6.1. Grouping and administration

60 ICR mice were randomly divided into 5 groups, 12 in each group: the control group, model group, positive drug group, raw WP group, and processed WP group. The treatment group was given the corresponding drug by intragastric administration, and the blank group and the model group were given the corresponding volume of normal saline for 14 consecutive days [14]. The specific dosage regimen is shown in Table 1. One hour after administration on the 14th day, the blank group was intraperitoneally injected with normal saline, and the mice in other groups were injected intraperitoneally with 0.5% carrageenan solution to establish a thrombus model (Fig. 1).

2.6.2. Thrombosis rate calculation

After 48 h of injecting carrageenan solution to establish the thrombus model (1 h after intragastric administration on the 16th day), the mice were anesthetized by inhalation of 2% isoflurane. The length of the tail thrombus and the total length of the mice's tail were measured with a steel ruler, and the relative length of the tail thrombus and the thrombus formation rate of the mice were calculated, respectively.

2.6.3. Plasma sample collection

After the photographing and measurement were completed, a centrifuge tube containing EDTA was used to collect the plasma sample collected from the mouse eyeball. Then, the centrifuge tube was gently inverted about 5 times to ensure the whole blood and the anticoagulant were mixed. After centrifugation at 3000 rpm at 4 °C for 10 min, the supernatant was collected and stored in a −80 °C refrigerator.

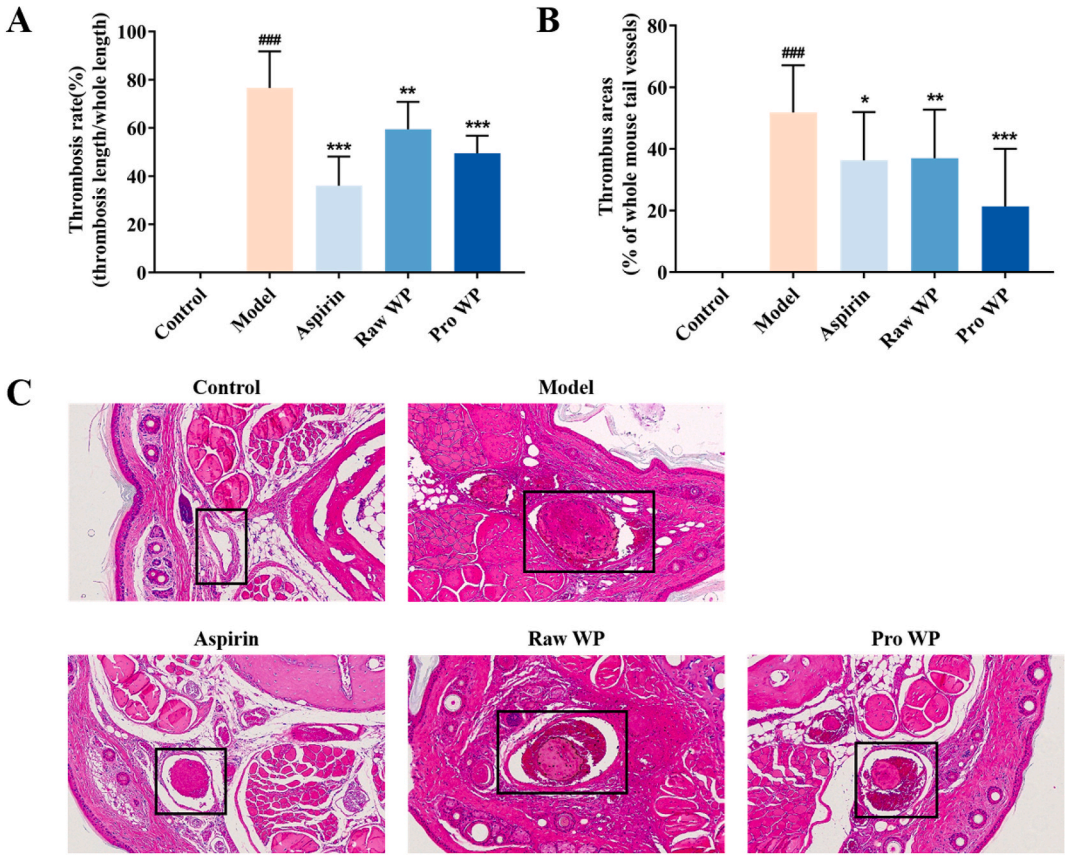

Fig. 2. Antithrombotic effects of the raw and processed WP. (A: Quantitative results of mouse tail vein thrombosis rate; B: Quantitative results of mouse tail vein thrombus area in the tail blood vessels percentage; C: A typical image of a paraffin section of the mouse tail at 4 cm from the tail tip (× 40, scale bar = 500 μm), the black box is a blood vessel, and the inside is a thrombus. $^{###}P < 0.001$ means the difference is statistically significant compared with the blank group; $^{***}P < 0.001$, $^{**}P < 0.01$, $^{*}P < 0.05$ means the difference is statistically significant compared with the model group).

2.6.4. Collection and evaluation of tail pathology tissue sections

The mice's tails were taken and fully fixed in 4% paraformaldehyde fixative for 48 h. After the tail samples were decalcified, the mouse tail paraffin pathological tissue sections were prepared 4 cm from the tail tip and stained with hematoxylin-eosin (H&E). The mice tail vessels were observed using Image-PRO PLUS 6.0 (Media Cybernetics, Inc., Rockville, MD, USA), the thrombus area was measured, and the percentage was calculated.

2.7. Metabolomics study in raw and processed WP

2.7.1. Plasma sample preparation

Plasma samples frozen at −80 °C were taken out and thawed at room temperature. Take 100 μL of plasma, add 300 μL of acetonitrile, sonicate in an ice-water bath for 10 min, vortex mix for 1 min, and centrifuge at 13000 rpm for 15 min at 4 °C. Take the supernatant into a pre-opened liquid phase vial for UPLC-Q-TOF/MS analysis.

2.7.2. QC sample preparation

Draw 10 μL of plasma from each sample into a centrifuge tube and vortex for 1 min. QC samples were prepared according to the above-mentioned "Plasma Sample Preparation," and 6 QC samples were processed in parallel for quality monitoring and methodological investigation during UPLC-Q-TOF/MS sample injection analysis.

2.7.3. Analysis conditions

2.7.3.1. Chromatographic conditions. The chromatographic column was ACQUITY UPLC BEH C18 (2.1 × 100 mm, 1.7 μm), with solvent A (0.1% formic acid in water) -solvent B (0.1% formic acid in acetonitrile) as the mobile phase. The elution gradient was (0–0.5 min, 1%B; 0.5–2 min, 1%-50%B; 2–9 min, 50%-99%B; 9–10 min, 99%B; 10–10.5 min, 99%-1%B; 10.5–12 min, 1%B); the column temperature was 40 °C; the flow rate was 0.3 mL/min; the injection volume was 5 μL. And QC samples were injected every 10 injections.

2.7.3.2. Mass spectrometer conditions. Electrospray ionization source (ESI source) was used for mass spectrometry detection and analysis in positive ionization mode. High-purity nitrogen was used as the auxiliary spray ionization desolvation gas. Drying gas flow rate 10 mL/min, nitrogen temperature 350 °C, atomizing gas pressure 310 kPa, desolvation nitrogen flow rate 600 L/h, cone backflush nitrogen 50 L/h, capillary ionization voltage 2.1 kV, capillary temperature 300 °C, the ion source temperature was 350 °C, and the mass spectrometry primary acquisition range was m/z 30–1000 Da.

2.7.4. Methodological investigation

2.7.4.1. Instrument precision test. Take the same QC sample solution, inject it 6 times continuously, and export the data as peak area. After 80% rounding and filling out the missing values, calculate the RSD value of each ion feature. It is required that the characteristic peaks with RSD<30% account for more than 70%.

2.7.4.2. Method repeatability test. Prepare 6 QC samples in parallel, inject and analyze continuously, and export the data as peak area. After 80% rounding and missing value filling, calculate the RSD value of each ion feature. It is required that the characteristic peaks with RSD<30% account for more than 70%.

2.7.4.3. Sample stability test. Take the same QC sample solution, inject, and analyze at 0, 4, 8, 10, 12, and 16 h respectively. And export the data as peak area. After 80% rounding and missing value filling, calculate the RSD value of each ion feature. It is required that the characteristic peaks with RSD<30% account for more than 70%.

2.8. Multivariate statistical analysis and differential metabolite identification

Data acquisition was performed using MassLynx v4.1 workstation (Waters Corp., Manchester, UK). Import all raw mass spectrum data into Progenesis QI software (Nonlinear Dynamics, 2014, version 1.0) for data processing, including peak extraction, peak alignment, peak matching, and normalization, and obtain a peak list containing information such as compound retention time, mass-to-charge ratio and peak intensity, and input to an Excel table for preprocessing. The 80% rule was applied to remove missing values,

Table 2
Detailed results of the methodological investigation in positive ion mode.

Category	Instrument precision	Method reproducibility	Sample stability
RSD<10%	36.82	32.18	26.55
10%≤RSD<20%	25.23	24.50	27.43
20%≤RSD<30%	12.54	13.38	16.07

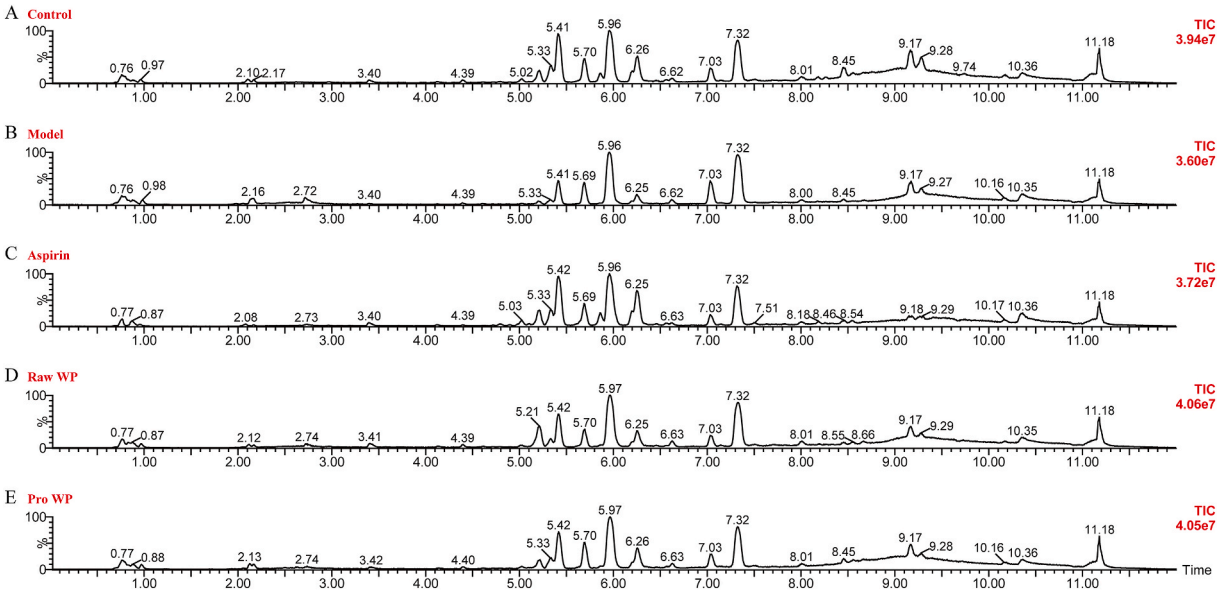

Fig. 3. Representative plasma TIC graphs of different groups. (A: the control group; B: the model group; C: the positive group; D: the raw WP group; E: the processed WP group).

peak filtering of the raw data was performed, and missing values still present were filled using the non-zero mean of the remaining samples in each group. The preprocessed data were imported into SIMCA-P 14.1 (Umetrics, Umea, Sweden) software for multivariate data analysis. Using unsupervised principal component analysis (PCA) to observe the samples' degree of aggregation and dispersion

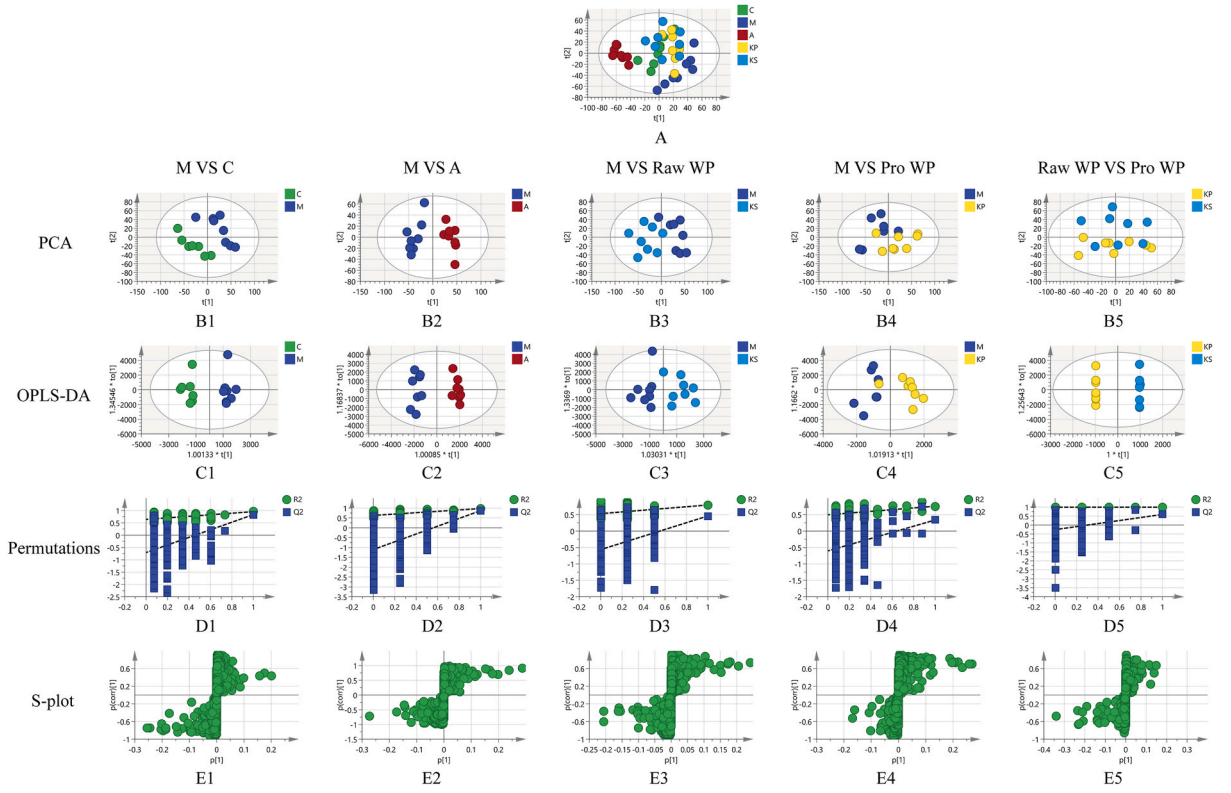

Fig. 4. Multivariate statistical analysis results. (A: PCA analysis chart of all groups in positive ion mode; B–D: Multivariate statistical analysis chart in positive ion mode; B: PCA analysis chart; C: OPLS-DA analysis chart; E: permutation test; F: S-plot analysis; 1: M VS C; 2: M VS A; 3: M VS Raw WP; 4: M VS Pro WP; 5: Raw WP VS Pro WP).

Table 3
Multivariate statistical analysis model parameters.

Category	Parameter	C VS M	M VS A	M VS Raw WP	M VS Pro WP	Raw WP VS Pro WP
PCA	R^2X	0.583	0.660	0.576	0.520	0.408
	Q^2	0.217	0.250	0.229	0.122	0.185
OPLS-DA	R^2X	0.767	0.629	0.434	0.518	0.958
	R^2Y	0.966	0.974	0.793	0.756	1.000
	Q^2	0.822	0.870	0.459	0.336	0.594
Permutations	R^2	(0.0, 0.822)	(0.0, 0.625)	(0.0, 0.523)	(0.0, 0.502)	(0.0, 0.1)
	Q^2	(0.0, −0.738)	(0.0, −1.100)	(0.0, −0.650)	(0.0, −0.516)	(0.0, −0.253)
	Hypothesis	200	200	200	200	200

and whether there are outliers. After removing outliers, supervised orthogonal partial least squares-discriminant analysis (OPLS-DA) was performed to evaluate the model's predictive ability. Among them, R^2X and R^2Y represent the interpretation rate of the built model to the X and Y matrices, and Q^2 represents the model's predictive ability. The closer the value is to 1, the better the model is. Then, use the permutation test (Permutation) to verify the reliability and stability of the model and judge whether the data is overfitting through the intercept of R^2 and Q^2. The important analysis value of the projection variable (VIP) obtained based on OPLS-DA was exported, and the peak list conforming to VIP>1 was imported into SPSS 25.0 software for statistical analysis. First, the Shapiro-Wilk test was used to judge whether the data conformed to the normal distribution. The data conforming to the normal distribution were subjected to the independent sample T-test, and the data not conforming to the normal distribution were subjected to the Mann-Whitney U nonparametric test. From a statistical point of view, the differential compounds with $P < 0.05$ were screened, and the compounds with VIP>1 and $P < 0.05$ were considered as differential metabolites and identified. Using Progenesis QI software and network open-source metabolite databases, such as HMDB (https://hmdb.ca/), PubChem (https://pubchem.ncbi.nlm.nih.gov/), KEGG (https://www.kegg.jp/), etc. to match secondary fragments, and calculate the error between the measured and theoretical values of molecular weight within 10 ppm to identify, screen and determine differential metabolites.

2.9. Metabolic pathway analysis

Import the identified differential metabolites into Metaboanalyst (https://www.metaboanalyst.ca/) for pathway enrichment analysis, screen metabolites with biological significance, and analyze the metabolic pathways of metabolite aggregation.

3. Results

3.1. Antithrombotic pharmacodynamic results in raw and processed WP

Compared with the blank group, the mice tails in each group after carrageenan injection appeared to have different lengths of thrombi. Among them, the thrombus in the model group was the longest and darkest, with an average thrombus formation rate of 76.61% ($P < 0.001$), indicating that the thrombus model was successfully established. The quantitative results of the tail vein thrombosis rate in each group are shown in Fig. 2A. Compared with the model group, the positive drug control group could significantly inhibit the formation of thrombus and reduce the rate of thrombus formation ($P < 0.001$). The relative length of the thrombus in the raw and processed WP was significantly shortened, which indicated that oral administration of the raw or processed WP could inhibit carrageenan-induced thrombus formation. And the inhibitory effect of the processed WP ($P < 0.001$) is more significant than that of the raw WP ($P < 0.01$), but there is no significant difference between the two.

The pathological tissue sections of the mice's tail veins were observed under an optical microscope. There was no thrombus in the blank group, and there was a large thrombus area in the tail vessel lumen of the model group. The thrombus area was significantly reduced in each treatment group (Fig. 2C). The reduction degree of thrombus area in the aspirin group was similar to the raw WP group. After oral administration of the raw and processed WP, the thrombus incidence decreased to 36.9% and 32.8%, respectively, both of which were significantly different from the model group. And the processed WP group ($P < 0.001$) was more significant than the raw WP group ($P < 0.01$), but there was no significant difference between the two groups (Fig. 2B). This result is consistent with the tail vein thrombus relative length, showing that high-temperature processing can enhance the WP's antithrombotic effect to a certain extent.

3.2. Antithrombotic metabolomics results in raw and processed WP

3.2.1. Methodological investigation results

The results show that in the positive ion mode, the characteristic peaks with chromatographic peak area RSD<30% in the investigation of instrument precision, method reproducibility, and sample stability accounted for 74.59%, 70.06%, and 70.05% of the total, all greater than 70%, which proves that the methodological investigation results are good. The specific results are shown in Table 2.

Table 4
Information of differential metabolites.

No.	RT (min)	Ion mode	Metabolite name	Caled *m/z*	Obsed *m/z*	Eorror ppm	Formula	MS/MS	C VS M	M VS A	M VS Raw WP	M VS Pro WP	Raw WP VS Pro WP
1	0.82	$[M+H]^+$	(S)-carnitinium	162.1130	162.1130	0.00	$C_7H_{16}NO_3$	58.0687, 60.0821, 85.0258	↑**	↑***	↑**	↑**	—
2	0.82	$[M+H]^+$	Triazophos	314.0723	314.0731	2.55	$C_{12}H_{16}N_3O_3PS$	168.1190, 181.0041, 239.9928, 257.0116, 259.0385	↓*	↑***	—	—	—
3	0.82	$[M+H]^+$	Phosphoribosylformylglycinamidine	314.0748	314.0731	−5.41	$C_8H_{16}N_3O_8P$	98.9872, 156.0203, 195.0046	↓*	↑***	—	—	—
4	0.82	$[M+H]^+$	5′-Phosphoribosyl-N-formylglycinamidine	314.0748	314.0731	-5.41	$C_8H_{16}N_3O_8P$	114.0653, 130.0475, 134.0816, 188.1098, 198.0835, 296.0645	↓*	↑***	—	—	—
5	0.82	$[M+H]^+$	L-Chlorozotocin	314.0748	314.0731	−5.41	$C_8H_{16}N_3O_8P$	60.0415, 88.0353, 152.0213, 192.0163, 194.0302, 206.0649, 222.0254, 278.0536	↓*	↑***	—	—	—
6	0.97	$[M+H]^+$	Uric acid	169.0356	169.0360	2.37	$C_5H_4N_4O_3$	43.0242, 69.0077, 71.0244, 83.0247, 97.0033, 126.0310, 151.0271, 169.0373	↓*	↑**	—	—	—
7	0.97	$[M+H]^+$	N-(3-Methylbut-2-EN-1-YL)-9H-purin-6-amine	204.1244	204.1240	−1.96	$C_{10}H_{13}N_5$	57.0715, 67.0559, 71.0870, 86.0960, 204.1265	↓*	↑***	↑**	↑*	—
8	0.97	$[M+H]^+$	Glutamic acid diethyl ester	204.1230	204.1240	4.90	$C_9H_{17}NO_4$	44.0469, 57.0385, 72.0436, 88.0721, 132.1020, 172.0995, 204.1265	↓*	↑***	↑**	↑*	—
9	0.97	$[M+H]^+$	1-Carboxyethylisoleucine	204.1230	204.1240	4.90	$C_9H_{17}NO_4$	44.0469, 69.0658, 71.0870, 72.0436, 86.0960, 97.0635, 140.1086, 158.1176, 204.1265	↓*	↑***	↑**	↑*	—
10	0.97	$[M+H]^+$	1-Carboxyethylleucine	204.1230	204.1240	4.90	$C_9H_{17}NO_4$	43.0528, 69.0658, 84.0823, 90.0541, 102.0558, 130.0874, 158.1160	↓*	↑***	↑**	↑*	—
11	0.97	$[M+H]^+$	Acetyl-DD-carnitine	204.1230	204.1240	4.90	$C_9H_{17}NO_4$	57.0385, 85.0298	↓*	↑***	↑**	↑*	—
12	0.97	$[M+H]^+$	LL-Acetylcarnitine	204.1230	204.1240	4.90	$C_9H_{17}NO_4$	57.0385, 85.0298	↓*	↑***	↑**	↑*	—
13	0.97	$[M+H]^+$	N-Lactoylleucine	204.1230	204.1240	4.90	$C_9H_{17}NO_4$	86.0960, 114.0933, 130.0874, 132.1020	↓*	↑***	↑**	↑*	—
14	0.97	$[M+H]^+$	DLDL-Acetylcarnitine	204.1230	204.1240	4.90	$C_9H_{17}NO_4$	57.0385, 85.0298	↓*	↑***	↑**	↑*	—
15	2.05	$[M+H]^+$	Isoindoline	120.0808	120.0814	5.00	C_8H_9N	91.0554, 103.0551	↓**	↑***	↑**	↑*	—
16	2.05	$[M+H]^+$	Indoline	120.0808	120.0814	5.00	C_8H_9N	39.0207, 77.0377, 91.0554, 94.0672, 103.0551, 118.0635	↓**	↑***	↑**	↑*	—
17	2.05	$[M+H]^+$	4-(4-Aminophenoxy)aniline	201.1022	201.1004	−8.95	$C_{12}H_{12}N_2O$	94.0630, 160.0766	↓**	↑***	↑**	↑**	—
18	2.15	$[M+H]^+$	Isoindole	118.0651	118.0655	3.39	C_8H_7N	65.0333, 75.0276, 91.0554, 118.0635	↓*	↑***	↑***	↑**	—
19	2.15	$[M+H]^+$	Benzeneacetonitrile	118.0651	118.0655	3.39	C_8H_7N	65.0333, 75.0276, 91.0554	↓*	↑***	↑***	↑**	—
20	2.15	$[M+H]^+$	Indole	118.0651	118.0655	3.39	C_8H_7N	65.0333, 75.0276, 118.0635	↓*	↑***	↑***	↑**	—
21	2.18	$[M+H]^+$	gamma-Glutamylisoleucine	261.1445	261.1448	1.15	$C_{11}H_{20}N_2O_6$	56.0470, 57.0616, 69.0694, 86.0960, 101.0701, 102.0514, 169.1395	↓*	↑***	↑**	↑**	—
22	2.18	$[M+H]^+$	gamma-Glutamylleucine	261.1445	261.1448	1.15	$C_{11}H_{20}N_2O_6$	56.047, 69.0694, 86.0960, 101.0701, 102.0514, 169.1395	↓*	↑***	↑**	↑**	—
23	2.23	$[M+H]^+$	Kelatorphan	295.1288	295.1293	1.69	$C_{14}H_{18}N_2O_5$	72.0436, 91.0554, 117.0646, 119.0857, 129.0387, 133.0673	↓**	↑***	↑**	↑***	—
24	2.23	$[M+H]^+$	Phenylalanylglutamic acid	295.1288	295.1293	1.69	$C_{14}H_{18}N_2O_5$	79.0551, 91.0554, 103.0551, 109.1029, 120.0836, 133.0673, 148.0744	↓**	↑***	↑**	↑***	—
25	2.23	$[M+H]^+$	Glutamylphenylalanine	295.1288	295.1293	1.69	$C_{14}H_{18}N_2O_5$	79.0551, 88.0721, 91.0554, 103.0551, 105.0683, 120.0836, 126.1241, 295.1261	↓**	↑***	↑**	↑***	—
26	2.23	$[M+H]^+$	Lidofenin	295.1288	295.1293	1.69	$C_{14}H_{18}N_2O_5$	88.0394, 90.0541, 91.0554, 105.0683, 118.0635, 120.0836,	↓**	↑***	↑**	↑***	—

(*continued on next page*)

Table 4 (*continued*)

No.	RT (min)	Ion mode	Metabolite name	Caled *m/z*	Obsed *m/z*	Eorror ppm	Formula	MS/MS	C VS M	M VS A	M VS Raw WP	M VS Pro WP	Raw WP VS Pro WP
								142.0638, 146.0623, 148.0797, 293.1194					
27	2.29	$[M+H]^+$	Valerylcarnitine	246.1700	246.1706	2.44	$C_{12}H_{23}NO_4$	57.0319, 71.0465, 85.0298	↓**	↑***	↑*	↑**	—
28	2.29	$[M+H]^+$	Pinacidil	246.1713	246.1706	−2.84	$C_{13}H_{19}N_5$	69.0730, 80.0520, 85.0580, 86.0970, 100.1111, 136.0810, 150.1002, 152.1129, 162.0771, 230.1461	↓**	↑***	↑*	↑**	—
29	2.29	$[M+H]^+$	Isovalerylcarnitine	246.1700	246.1706	2.44	$C_{12}H_{23}NO_4$	57.0319, 71.0465, 85.0298	↓**	↑***	↑*	↑**	—
30	2.29	$[M+H]^+$	2-Methylbutyroylcarnitine	246.1700	246.1706	2.44	$C_{12}H_{23}NO_4$	57.0319, 71.0465, 85.0298	↓**	↑***	↑*	↑**	—
31	2.46	$[M+H]^+$	PGP(5-iso PGF2VI/i-14:0)	845.4212	845.4158	−6.39	$C_{38}H_{70}O_{16}P_2$	43.0557, 57.0616, 71.0870, 119.0857, 593.4460	↓***	↑***	↑*	↑*	—
32	2.46	$[M+H]^+$	PGP(PGD1/i-12:0)	845.4212	845.4158	−6.39	$C_{38}H_{70}O_{16}P_2$	43.0557, 57.0616, 71.0870, 119.0857, 593.4460	↓***	↑***	↑*	↑*	—
33	2.46	$[M+H]^+$	PGP(PGE1/i-12:0)	845.4212	845.4158	−6.39	$C_{38}H_{70}O_{16}P_2$	43.0557, 57.0616, 71.0870, 119.0857, 593.4460	↓***	↑***	↑*	↑*	—
34	2.65	$[M+H]^+$	PIP(PGF1alpha/22:2)	1071.5781	1071.5852	6.63	$C_{51}H_{92}O_{19}P_2$	57.0649, 71.0870, 81.0670, 101.0921	↓**	↑*	—	—	—
35	4.15	$[M+H]^+$	(2R,3R)-2-Aminooctadecane-1,3-diol	302.3054	302.3063	2.98	$C_{18}H_{39}NO_2$	41.0372, 43.0557, 44.0469, 57.0616, 60.0449, 69.0694, 71.0833, 83.0883, 97.1022, 102.0911, 116.1075, 144.1373, 158.1545	↑*	↓***	↓***	↓**	—
36	4.15	$[M+H]^+$	Sphinganine	302.3054	302.3063	2.98	$C_{18}H_{39}NO_2$	60.0449, 67.0523, 83.0883, 97.1022, 109.1029, 240.2634, 284.0913	↑*	↓***	↓***	↓**	—
37	4.39	$[M+H]^+$	Indane	119.0855	119.0857	1.68	C_9H_{10}	91.0554, 117.0693, 119.0857	↑**	—	↓**	↓**	—
38	4.90	$[M+H]^+$	Ganoderic acid A	517.3160	517.3171	2.13	$C_{30}H_{44}O_7$	113.0928, 157.0856, 343.2284, 367.2295, 385.2760, 481.2927, 517.3168	↑**	—	↓*	↓*	—
39	4.90	$[M+H]^+$	Ganoderic acid B	517.3160	517.3171	2.13	$C_{30}H_{44}O_7$	113.0928, 139.0769,343.2284, 367.2295, 481.2927, 517.3168	↑**	—	↓*	↓*	—
40	4.90	$[M+H]^+$	Cucurbitacin D	517.3160	517.3171	2.13	$C_{30}H_{44}O_7$	303.1989, 343.2284, 481.2927, 517.3168	↑**	—	↓*	↓*	—
41	4.90	$[M+H]^+$	Ganoderic acid epsilon	517.3160	517.3171	2.13	$C_{30}H_{44}O_7$	113.0928, 139.0769,343.2284, 367.2295, 481.2927, 517.3168	↑**	—	↓*	↓*	—
42	4.90	$[M+H]^+$	Ganoderic acid delta	517.3160	517.3171	2.13	$C_{30}H_{44}O_7$	113.0928, 139.0769,343.2284, 367.2295, 481.2927, 517.3168	↑**	—	↓*	↓*	—
43	4.90	$[M+H]^+$	Ganoderenic acid C	517.3160	517.3171	2.13	$C_{30}H_{44}O_7$	139.0769,343.2284, 367.2295, 481.2927, 517.3168	↑**	—	↓*	↓*	—
44	5.14	$[M+H]^+$	Estradiol enanthate	385.2737	385.2743	1.56	$C_{25}H_{36}O_3$	43.0585, 57.0682, 91.0554, 95.0863, 237.1671, 265.2167, 273.1826, 277.2170, 327.1936, 329.2186, 385.2760	↑**	↓**	↓**	↓**	—
45	5.14	$[M+H]^+$	Persicachrome	385.2737	385.2743	1.56	$C_{25}H_{36}O_3$	95.0863,107.0874, 117.0693, 119.0857, 131.0852, 147.1143, 173.1320, 183.1190, 187.1468, 273.1826, 365.2408	↑**	↓**	↓**	↓**	—
46	5.14	$[M+H]^+$	Persicaxanthin	385.2737	385.2743	1.56	$C_{25}H_{36}O_3$	73.1320, 119.0857, 121.1001, 145.1035, 187.1469, 271.1657, 273.1826, 365.2408, 385.2760	↑**	↓**	↓**	↓**	—
47	5.17	$[M+H]^+$	25-Cinnamoyl-vulgaroside	567.3316	567.3333	3.00	$C_{34}H_{46}O_7$	79.0551, 91.0554, 115.0561, 133.0623, 137.1322, 163.0736	↑***	↓***	↓**	↓**	—

(*continued on next page*)

Table 4 (*continued*)

No.	RT (min)	Ion mode	Metabolite name	Caled *m/z*	Obsed *m/z*	Eorror ppm	Formula	MS/MS	C VS M	M VS A	M VS Raw WP	M VS Pro WP	Raw WP VS Pro WP
48	5.21	$[M+H]^+$	Phosphorylcholine	184.0739	184.0743	2.17	$C_5H_{15}NO_4P$	60.0821, 84.0863, 124.9988, 184.0775	↑***	↓***	↓**	↓**	—
49	5.21	$[M+H]^+$	Phytolaccatoxin	519.3316	519.3344	5.39	$C_{30}H_{46}O_7$	165.0926, 185.1156, 319.1953, 453.2921	↑**	↓***	↓**	↓**	—
50	5.21	$[M+H]^+$	Corosin	519.3316	519.3344	5.39	$C_{30}H_{46}O_7$	57.0352, 373.2700, 453.2921	↑**	↓***	↓**	↓**	—
51	5.21	$[M+H]^+$	Perulactone	519.3316	519.3344	5.39	$C_{30}H_{46}O_7$	55.0544, 271.2016, 439.2816	↑**	↓***	↓**	↓**	—
52	5.21	$[M+H]^+$	Ganoderic acid C2	519.3316	519.3344	5.39	$C_{30}H_{46}O_7$	41.0372, 71.0465, 85.0620, 369.2655, 373.2700	↑**	↓***	↓**	↓**	—
53	5.21	$[M+H]^+$	Ganolucidic acid C	519.3316	519.3344	5.39	$C_{30}H_{46}O_7$	41.0372, 71.0465, 85.0620, 369.2655, 373.2700	↑**	↓***	↓**	↓**	—
54	5.24	$[M+H]^+$	Arachidoyl Ethanolamide	356.3523	356.3528	1.40	$C_{22}H_{45}NO_2$	45.0376, 55.0577, 57.2597, 69.0694, 83.0843, 95.0863, 132.1025, 338.3440	↑***	↓***	↓***	↓***	—
55	5.38	$[M+H]^+$	Laprafylline	501.2973	501.2965	−1.60	$C_{29}H_{36}N_6O_2$	83.0843, 91.0554, 117.0693, 196.1158, 198.1265, 345.2049	↑*	↓*	↓*	↓*	—
56	6.00	$[M+H]^+$	Janthitrem C	570.3578	570.3557	−3.68	$C_{37}H_{47}NO_4$	41.0344, 55.0544, 57.0352, 293.2165, 303.1989, 512.3140	↑***	↓**	↓*	↓*	—
57	5.87	$[M+H]^+$	Hovenidulcigenin A	545.3473	545.3493	3.67	$C_{32}H_{48}O_7$	85.0218, 153.1270, 225.2247, 235.2077, 439.2816, 487.3076, 545.3436	↑**	↓**	↓*	↓*	—
58	6.00	$[M+H]^+$	LysoPC(22:5/0:0)	570.3554	570.3557	0.53	$C_{30}H_{52}NO_7P$	86.0960, 104.1082, 387.2841, 393.3962	↑***	↓**	↓*	↓*	—
59	6.25	$[M+H]^+$	Tridodecylamine	522.5972	522.5983	2.10	$C_{36}H_{75}N$	43.0585, 71.0870, 85.1023, 450.5077	↑**	↓***	↓**	↓**	—
60	6.27	$[M+H]^+$	LysoPE(P-16:0/0:0)	438.2979	438.2980	0.23	$C_{21}H_{44}NO_6P$	42.0305, 96.9689, 113.1346, 127.1412, 198.0589, 223.2437, 283.2616	↓**	↑***	—	—	—
61	6.34	$[M+H]^+$	Ganodermic acid P2	571.3629	571.3638	1.58	$C_{34}H_{50}O_7$	267.2295, 553.3565, 571.3616	↑**	↓**	↓**	↓**	—
62	6.34	$[M+H]^+$	Ganoderic acid Mk	571.3629	571.3638	1.58	$C_{34}H_{50}O_7$	111.0498, 125.0525, 139.0769, 349.2158, 353.2417, 399.2848, 467.3527, 493.3308, 541.3541, 571.3616	↑**	↓**	↓**	↓**	—
63	6.56	$[M+H]^+$	Hovenidulcigenin B	547.3629	547.3635	1.10	$C_{32}H_{50}O_7$	69.0694, 87.0426, 115.0701, 153.1270, 283.1513, 431.3109, 487.3462	↑**	↓**	↓**	↓**	—
64	6.57	$[M+H]^+$	Theasapogenol A	507.3680	507.3692	2.37	$C_{30}H_{50}O_6$	137.0964, 153.0999, 291.2386, 333.2076, 459.3452, 507.3649	↑**	↓**	↓**	↓**	—
65	6.86	$[M+H]^+$	DG(PGJ2/0:0/8:0)	535.3629	535.3638	1.68	$C_{31}H_{50}O_7$	71.0833, 83.0883, 97.1022, 371.2088, 447.2792	↑*	↓**	↓**	↓**	—
66	7.82	$[M+H]^+$	Laurdan	354.2791	354.2767	−6.77	$C_{24}H_{35}NO$	57.0682, 71.0833, 95.0863, 172.1109, 284.2029, 334.2524	↑***	↓***	—	—	—

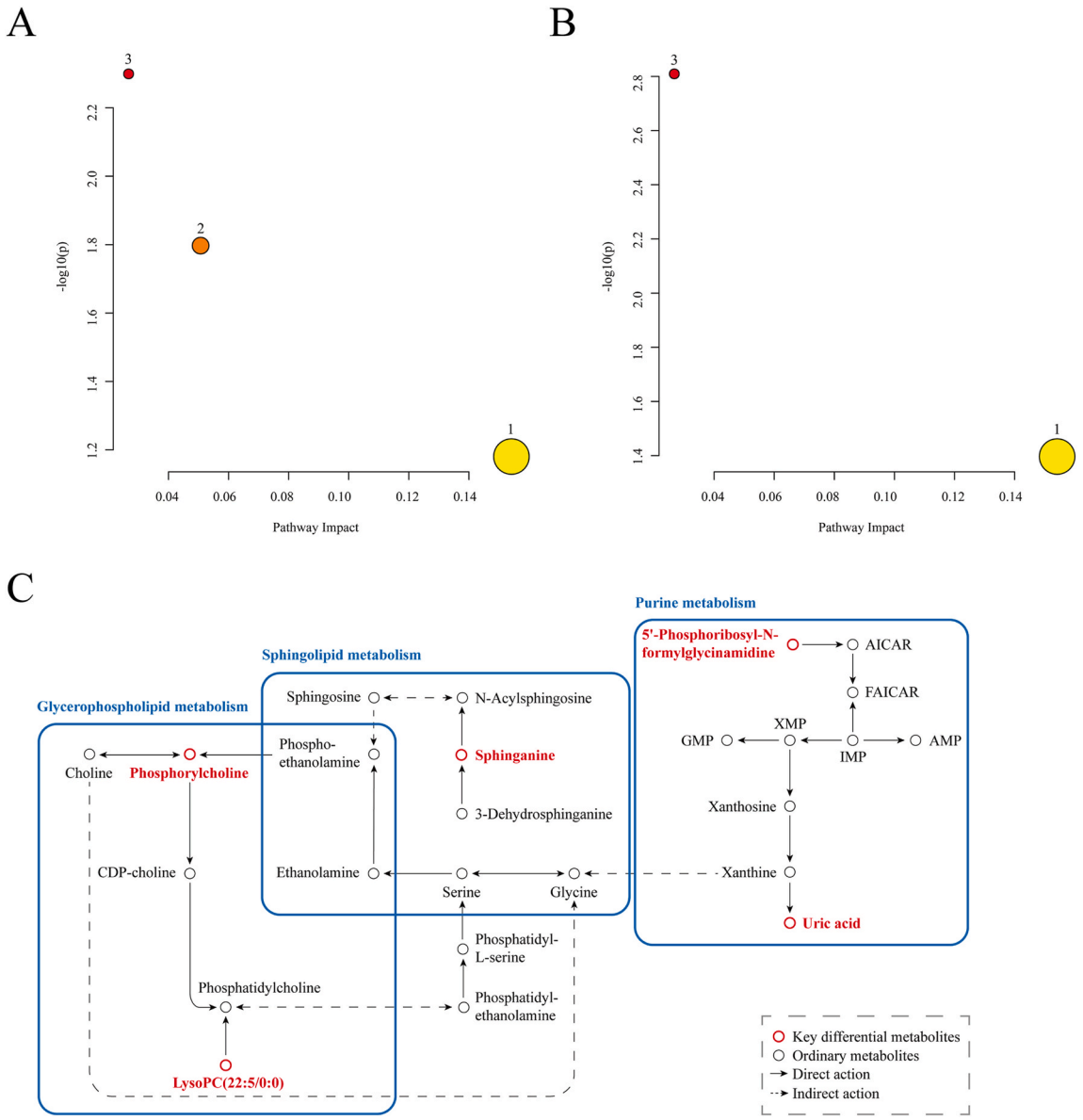

Fig. 5. Enrichment results of differential metabolite pathways. (A: M VS C and M VS A pathway enrichment analysis diagram; B: M VS Raw WP and M VS Pro WP pathway enrichment analysis diagram; C: biomarker metabolic pathway mechanism diagram).

Table 5
Metabolic pathways of biomarkers.

No.	Pathway Name	C VS M & M VS A Impact	M VS Raw WP & M VS Pro WP Impact
1	Sphingolipid metabolism	0.15416	0.15416
2	Purine metabolism	0.0507	–
3	Glycerophospholipid metabolism	0.02673	0.02673

3.2.2. Multivariate statistical analysis

The UPLC-Q-TOF/MS mass spectrometer was used to conduct non-targeted metabolomics research on mouse plasma. The QC samples extracted from Masslynx and the TIC diagrams of each group are shown in Fig. 3A–E. Metabolomics analysis was performed using multivariate statistical analysis methods such as PCA, OPLS-DA, and the permutation test. The number of permutation test hypothesis tests is set to 200.

First, PCA analysis was performed on the data of all groups in positive ion mode (Fig. 4A). The control group, the model group, the positive drug group, the raw WP group, and the processed WP group were respectively gathered together. Still, the aggregation effect of the raw WP group was not as good as that of other groups. Afterwards, the model and the control groups were analyzed by PCA and OPLS-DA (Fig. 4B1 and C1). It can be observed that the model group and the control group samples are significantly separated, indicating that the levels of certain metabolites in the body change under pathological conditions. PCA and OPLS-DA analysis was performed on the positive group, the raw WP group, the processed WP group, and the model group, respectively (Fig. 4B2-B5 and C2–C5). It can be seen from the figure that the positive drug and the samples of each administration group and the model group can be clearly distinguished, indicating that the drug can recall the metabolite level in the pathological state.

In the OPLS-DA model, Q^2 represents the prediction rate of the model; R^2 and Q^2 in the permutation test can be used to verify the model's accuracy. The R^2 and Q^2 of the OPLA-DA model established in this experiment all meet the requirements, the permutation test results are good (Fig. 4D1-D5), S-plot shows that the model can effectively screen important metabolites (Fig. 4E1-E5), and the model is reliable. The specific parameters are shown in Table 3.

3.2.3. Screening and identification of differential metabolites

Variables were screened according to the VIP values of the OPLS-DA model. The model group was compared with the blank group, with VIP>1 as the standard; the data was imported into SPSS 25.0 software for the normality test, independent sample T-test and non-parametric test, and compounds that met VIP>1 and $P < 0.05$ were screened.

Determine the molecular formula of the compound based on the retention time, accurate mass, and additive ion form in the peak list. The number of theoretical fragments was retrieved from the HMDB online database and related literature and compared with the original data secondary fragments to screen and identify differential metabolites and observe the content changes between groups. The analysis showed that 66 differential metabolites were identified in the model group compared to the control group. Compared with the model group, 59 differential metabolites were identified in the positive group; 58 differential metabolites were identified in both the raw and processed WP, and there was no significant difference between the two groups. The specific identification results and detailed information are shown in Table 4.

3.2.4. Metabolic pathway analysis

MetaboAnalyst5.0 was used to perform pathway enrichment analysis on the identified differential metabolites (Fig. 5A-B and Table 5). Compared between the control group and the model group and between the model group and the positive group, the metabolic pathways involved mainly include Sphingolipid metabolism, Purine metabolism, and Glycerophospholipid metabolism. Comparing the model group with the WP group (including the raw WP group and the processed WP group), only two metabolic pathways involved mainly include Sphingolipid metabolism and Glycerophospholipid metabolism. Based on the above results and KEGG pathway analysis, the biomarker metabolic pathway mechanism was obtained (Fig. 5C).

4. Discussion

Thrombosis is the main cause of cardiovascular and cerebrovascular diseases [15]. The formation of a thrombus is regulated by many factors, among which the complex signaling network of coagulation function and platelet activation function are key factors [16]. In this study, we found that WP's raw and processed products can significantly inhibit carrageenan-induced tail thrombosis in mice after intragastric administration for the first time. And the antithrombotic effect after high-temperature processing is more obvious than raw products. In order to better elucidate the antithrombotic effect of WP, the action mechanism was preliminarily discussed based on the plasma metabolomics research results. We found that small molecule metabolites in the metabolic pathways of Sphingolipid metabolism and Glycerophospholipid metabolism may play an important role. Studies have shown that changes in Sphingolipid metabolism pathway and Glycerophospholipid metabolism pathway are closely related to cardiovascular diseases [17]. Phosphatidylcholine and Sphingomyelin in plasma, the two most abundant phospholipids in mammalian plasma, have been considered risk factors for coronary heart disease [18,19]. Sphingolipid metabolism is involved in affecting the procoagulant activity of tissue factor (TF) and platelet autophagy and activation [20], and abnormal platelet activation can lead to thrombus formation [21]. Platelets also release a large amount of sphingosine-1-phosphate (S1P) during the coagulation process, or when thrombin is activated [22], S1P can participate in the cell signal transduction related to thrombus and is an important signaling lipid in -thrombus formation [23]. Sphinganine identified in this study is the precursor of S1P, and the interaction between the two can promote a new mechanism formation in Sphingolipid metabolism and thrombin generation [24].

According to the up and down regulation information of the differential metabolites identified among the groups in Table 2, compared with the model group, most differential metabolite level trends after administration of the raw and processed WP were consistent with those of the positive group, and even their effects were comparable to aspirin. However, after pathway enrichment, it was found that the participation of Purine metabolism was missing in the WP group compared with the positive drug group. The unidentified Uric acid in the WP group is the final product of the Purine metabolism process, and the Uric acid levels in serum are closely related to the increased risk of thrombosis recurrence [25]. In addition, the antithrombotic pharmacodynamics experiments in this study showed that the processed WP group can inhibit carrageenan-induced thrombosis better than the raw WP group. However, there were not many differences in the differential metabolites and metabolic pathways among the groups. We performed hierarchical clustering analysis on all differential metabolites to explore the possible reasons for this phenomenon and intuitively show the changes in differential metabolites among the groups. The depth of the color in the hierarchical cluster analysis graph reflects the size of the variable value, and the distance of the variable information in the vertical axis represents the similarity of the metabolite information

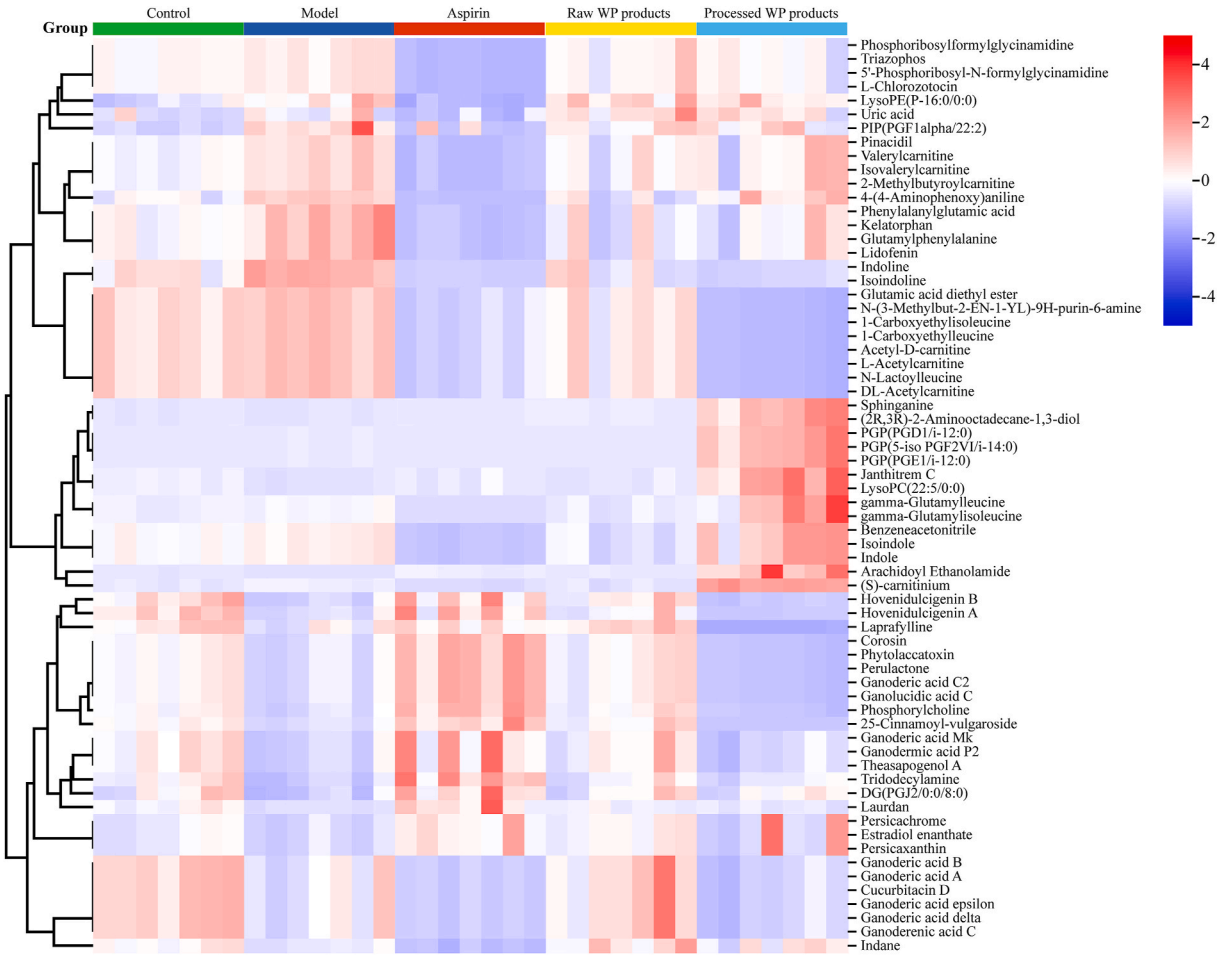

Fig. 6. Heatmap of differential metabolites between groups. Different colors in the heat map represent different relative content of metabolites; red represents relatively high content, and blue represents relatively low content. (For interpretation of the references to color in this figure legend, the reader is referred to the Web version of this article.)

(Fig. 6). We can clearly see that the types of small-molecule metabolites regulated between aspirin and WP are obviously different. After aspirin administration, the main changes are the small-molecule organic acid esters. However, after the administration of WP, the fluctuations of amino acids, lipids, and steroids were mainly manifested. In addition, these types of ingredients in the processed WP are also quite different from the raw WP, such as gamma-Glutamylleucine, Perulactone, etc.

As an animal traditional Chinese medicine, leech contains a lot of fat, protein, and steroid compounds. Steroids are the basis of hormone production and an important source of many life activities in the body [26]. Cholesterol is the most abundant steroid compound. Excessive plasma cholesterol levels and excessive cholesterol oxidation products can affect the human cardiovascular system [27]. WP is a non-blood-sucking leech, and its body mainly contains protein and polypeptide components rather than hirudin. After processing the wide-bodied golden leeches with talcum powder at a temperature above 200 °C, the chemical composition in the body will change significantly. Water-soluble proteins within the body undergo denaturation through the release of proteases, transforming into free amino acids or small molecule peptides. After high-temperature treatment processing, the composition of steroids and cholesterol oxidation products may also change significantly [28]. Studies have shown that the total amount of amino acids and the total amount of essential amino acids in the human body increase after leeches are scalded with talcum powder, and they are superior to raw products in terms of anti-inflammation and adjustment of serum high-density lipoprotein subcomponent ratios in hyperlipidemic animals [29]. In addition, leeches were powdered and administered orally in this study, and the small molecular polypeptide components produced by the changes in the chemical composition of the processed WP group may be more easily digested and degraded into small molecular metabolites by the gastrointestinal tract, thereby exerting the medicinal effect. Therefore, we believe that the increase or change of small molecular metabolites due to high-temperature processing, gastrointestinal digestion, and degradation may be one of the reasons why the processed WP group has better efficacy than the raw WP group. However, the relationship between the different components and the mechanism of anticoagulant and thrombolytic effects *in vivo* requires further verification and discussion in follow-up experiments. In addition, leeches contain many protein and polypeptide substances, and thrombus formation is closely related to the participation of multiple coagulation factors and thrombin. In the future, computer

simulation technology, proteomics, and other research can be carried out to explore better the antithrombotic activity of WP's raw and processed products. It provides a research basis for the correct processing and clinically rational drug use of animal traditional Chinese medicines such as WP.

5. Conclusions

This study investigated the *in vivo* antithrombotic activity of both the raw WP products and its talcum powder processed products, and the metabolomics technology was used to reveal the changes of small molecule metabolites *in vivo*. The results of pharmacodynamics showed that both the raw WP and its talcum powder processed products could inhibit the thrombosis induced by carrageenan in the mice tail vein, significantly reducing the thrombosis rate and thrombus area. The antithrombotic effect of the processed WP talcum powder was more obvious than the raw, but there was no significant difference between the two groups. The results of plasma metabolomics showed that after the administration of raw and processed WP, there was a tendency to reverse the metabolites in the model group mice. However, there was no significant difference between the two groups. The changes in small molecule metabolites, such as amino acids and lipids, in the body after administration were related to Sphingolipid metabolism and Glycerophospholipid metabolism. Therefore, processed WP will not reduce its antithrombotic activity. The reason why it is more effective than raw products may be related to the increase or change of small molecule metabolites produced after high-temperature processing and digestion and degradation in the gastrointestinal tract. This study provides a research basis for the subsequent research on the anticoagulant and thrombolytic activity of WP and a theoretical basis for the correct processing and clinically rational drug use of traditional animal Chinese medicines such as WP.

Funding

This work was supported by the National Natural Science Foundation of China (No. 82173955).

Ethics statement

This study was reviewed and approved by the Animal Ethics Committee of Beijing University of Chinese Medicine, with the approval number: No. BUCM-4-2022010102-1109, No. BUCM-4-2022010103-1110.

Data availability statement

Data will be made available on request. The data related to our research have been deposited in publicly available repositories. These databases include HMDB (https://hmdb.ca/), PubChem (https://pubchem.ncbi.nlm.nih.gov/), KEGG (https://www.kegg.jp/), and Metaboanalyst (https://www.metaboanalyst.ca/).

CRediT authorship contribution statement

Hongqian Kui: Writing – original draft, Methodology, Formal analysis, Data curation. **Yan Lei:** Methodology, Investigation. **Chunxue Jia:** Formal analysis, Data curation. **Quancheng Xin:** Formal analysis, Data curation. **Rustam Tursun:** Writing – review & editing, Investigation. **Miao Zhong:** Methodology, Conceptualization. **Chuanxin Liu:** Supervision, Project administration, Methodology. **Ruijuan Yuan:** Writing – original draft, Methodology, Funding acquisition, Conceptualization.

Declaration of competing interest

The authors declare that they have no known competing financial interests or personal relationships that could have appeared to influence the work reported in this paper.

Appendix A. Supplementary data

Supplementary data to this article can be found online at https://doi.org/10.1016/j.heliyon.2024.e27828.

References

[1] N.P. Committee, Pharmacopoeia of the People's Republic of China, China Medical Science and Technology Press, Beijing, 2020 (in Chinese).
[2] X. Wang, M. Niu, S.N. Wu, H.W.Y. Hu, X.Y. Liu, S.Y. Ma, et al., Leeches attenuate blood hyperviscosity and related metabolic disorders in rats differently than aspirin, J. Ethnopharmacol. 238 (2019) 111813, https://doi.org/10.1016/j.jep.2019.03.040.
[3] X.P. Tang, M.R. Chen, Z.L. Duan, J. Mwangi, P.P. Li, R. Lai, Isolation and characterization of poecistasin, an anti-thrombotic antistasin-type serine protease inhibitor from leech poecilobdella manillensis, Toxins 10 (11) (2018), https://doi.org/10.3390/toxins10110429.
[4] X. Liu, C.H. Wang, X. Ding, X.D. Liu, Q. Li, Y. Kong, A novel selective inhibitor to thrombin-induced platelet aggregation purified from the leech Whitmania pigra, Biochem. Biophys. Res. Commun. 473 (1) (2016) 349–354, https://doi.org/10.1016/j.bbrc.2016.03.117.

[5] S.S. Li, L. Cheng, D.K. An, S.L. Song, H. Liang, F.L. Chu, et al., *Whitmania pigra* Whitman extracts inhibit lipopolysaccharide induced rat vascular smooth muscle cells migration and their adhesion ability to THP-1 and RAW 264.7 cells, J. Atheroscler. Thromb. 24 (3) (2017) 301–311, https://doi.org/10.5551/jat.36558.
[6] S.M. Malinconico, J.B. Katz, A.Z. Budzynski, Hementin: anticoagulant protease from the salivary gland of the leech Haementeria ghilianii, J. Lab. Clin. Med. 103 (1) (1984) 44–58.
[7] A.M. Chudzinski-Tavassi, E.M. Kelen, A.P. de Paula Rosa, S. Loyau, C.A. Sampaio, C. Bon, et al., Fibrino(geno)lytic properties of purified hementerin, a metalloproteinase from the leech Haementeria depressa, Thromb. Haemost. 80 (1) (1998) 155–160.
[8] M. Salzet, V. Chopin, J. Baert, I. Matias, J. Malecha, Theromin, a novel leech thrombin inhibitor, J. Biol. Chem. 275 (40) (2000) 30774–30780, https://doi.org/10.1074/jbc.M000787200.
[9] K.W. Zhang, Y.J. Zhong, H.H. Cao, T. Lu, L. W, Y. Gao, C.Q. Mao, Quality analysis of Hirudo before and after processing, Chin. Tradit. Pat. Med. 40 (10) (2018) 2244–2249 (in Chinese).
[10] M. Zhong, Y. Lei, H. Tan, X.F. Wang, J.W. Hou, H.L. Xie, et al., In vitro anticoagulant activity of different processed products of poecilobdella manillensis by water extraction and bionic extraction (in Chinese), Modern Chin, Med 22 (3) (2020) 379–383+397.
[11] Y.J. Zhang, R. Yang, L.W. Wang, Y. Li, J. Han, Y.Y. Yang, et al., Purification and characterization of a novel thermostable anticoagulant protein from medicinal leech Whitmania pigra Whitman, J. Ethnopharmacol. 288 (2022), https://doi.org/10.1016/j.jep.2022.114990.
[12] Y. Shan, J.Z. Zhang, Y.Z. Ding, M.T. He, X.X. Dai, X.H. Ma, et al., In vitro anticoagulant activity of different processed products of Whitmania pigra by water extraction and bionic extraction (in Chinese), Chin, J. Chin. Mater. Med. 41 (10) (2016) 1843–1848.
[13] Q.Y. Huang, Q. Gao, X.X. Chai, W. Ren, G.F. Zhang, Y.J. Kong, et al., A novel thrombin inhibitory peptide discovered from leech using affinity chromatography combined with ultra-high performance liquid chromatography-high resolution mass spectroscopy, J. Chromatogr. B. 1151 (2020), https://doi.org/10.1016/j.jchromb.2020.122153.
[14] C. Wang, Z.S. Yuan, J.Q. Xie, Y. Lei, Y.H. Li, J.M. Huang, et al., Integrated metabolomics and molecular docking reveal berberrubine inhibits thrombosis by regulating the vitamin K catalytic cycle in mice, Eur. J. Pharmacol. 938 (2023) 175436, https://doi.org/10.1016/j.ejphar.2022.175436.
[15] B. Engelmann, S. Massberg, Thrombosis as an intravascular effector of innate immunity, Nat. Rev. Immunol. 13 (1) (2013) 34–45, https://doi.org/10.1038/nri3345.
[16] A.V. Belyaev, J.L. Dunster, J.M. Gibbins, M.A. Panteleev, V. Volpert, Modeling thrombosis in silico: frontiers, challenges, unresolved problems and milestones, Phys. Life Rev. 26–27 (2018) 57–95, https://doi.org/10.1016/j.plrev.2018.02.005.
[17] V.T. Dang, A. Huang, L.H. Zhong, Y.Y. Shi, G.H. Werstuck, Comprehensive plasma metabolomic analyses of atherosclerotic progression reveal alterations in glycerophospholipid and sphingolipid metabolism in apolipoprotein e-deficient mice, Sci. Rep. 6 (2016) 35037, https://doi.org/10.1038/srep35037.
[18] X.C. Jiang, F. Paultre, T.A. Pearson, R.G. Reed, C.K. Francis, M. Lin, et al., Plasma sphingomyelin level as a risk factor for coronary artery disease, Arterioscler. Thromb. Vasc. Biol. 20 (12) (2000) 2614–2618, https://doi.org/10.1161/01.atv.20.12.2614.
[19] W.H.W. Tang, Z.E. Wang, B.S. Levison, R.A. Koeth, E.B. Britt, X.M. Fu, et al., Intestinal microbial metabolism of phosphatidylcholine and cardiovascular risk, N. Engl. J. Med. 368 (17) (2013) 1575–1584, https://doi.org/10.1056/NEJMoa1109400.
[20] J. Wang, S. Keshava, K. Das, R. Kolesnick, X.C. Jiang, U.R. Pendurthi, et al., Alterations to sphingomyelin metabolism affect hemostasis and thrombosis, Arterioscler. Thromb. Vasc. Biol. 43 (1) (2023) 64–78, https://doi.org/10.1161/ATVBAHA.122.318443.
[21] M. Koupenova, B.E. Kehrel, H.A. Corkrey, J.E. Freedman, Thrombosis and platelets: an update, Eur. Heart J. 38 (11) (2017) 785–791, https://doi.org/10.1093/eurheartj/ehw550.
[22] T. Hla, S. Galvani, S. Rafii, R. Nachman, S1P and the birth of platelets, J. Exp. Med. 209 (12) (2012) 2137–2140, https://doi.org/10.1084/jem.20122284.
[23] L. Zhang, M. Orban, M. Lorenz, V. Barocke, D. Braun, N. Urtz, et al., A novel role of sphingosine 1-phosphate receptor S1pr1 in mouse thrombopoiesis, J. Exp. Med. 209 (12) (2012) 2165–2181, https://doi.org/10.1084/jem.20121090.
[24] T.Y. Lee, W.J. Lu, C.A. Changou, Y.C. Hsiung, N.T.T. Trang, C.Y. Lee, et al., Platelet autophagic machinery involved in thrombosis through a novel linkage of AMPK-MTOR to sphingolipid metabolism, Autophagy 17 (12) (2021) 4141–4158, https://doi.org/10.1080/15548627.2021.1904495.
[25] L. De Lucchi, C. Nardin, A. Sponchiado, D. Raggi, E. Faggin, E. Martini, et al., Serum uric acid levels and the risk of recurrent venous thromboembolism, J. Thromb. Haemost. 19 (1) (2021) 194–201, https://doi.org/10.1111/jth.15139.
[26] T.J. Cole, K.L. Short, S.B. Hooper, The science of steroids, Semin. Fetal Neonatal Med. 24 (3) (2019) 170–175, https://doi.org/10.1016/j.siny.2019.05.005.
[27] J.A.S. Carson, A.H. Lichtenstein, C.A.M. Anderson, L.J. Appel, P.M. Kris-Etherton, K.A. Meyer, et al., Dietary cholesterol and cardiovascular risk: a science advisory from the American Heart Association, Circulation 141 (3) (2020) e39–e53, https://doi.org/10.1161/CIR.0000000000000743.
[28] S.Z. Xu, Study of the changes of chemical composition of leech after processing, Shanxi J. Tradit. Chin. Med. 39 (7) (2018) 980–982 (in Chinese).
[29] X.R. Fan, Effect of processing on amino acid composition of leech (in Chinese), Strait, Pharm. J. (4) (2000) 44–45.